

Supplementary Document for Amulet

1. Performance on the SED dataset

The SED [1] dataset contains two subsets: SED1 and SED2. The SED1 has 100 images each containing only one salient object, while the SED2 has 100 images each containing two salient objects.

Tab. 1 provides the results of F-measure and MAE on the SED dataset. Fig. 1(a) and Fig. 1(b) show the PR curves on the SED1 and SED2 subset, respectively.

Both the F-measure in Tab. 1 and the PR curves in Fig. 1 show that our Amulet consistently outperforms other methods with a considerable margin. In addition, our Amulet performs much better on the complex SED2 subset, which has two salient objects.

2. PR curves on the DUT-OMRON and SOD datasets

The DUT-OMRON [13] dataset has 5,168 high quality images. This dataset is difficult and challenging, and provides more space of improvement for related research in saliency detection.

The SOD [12] dataset has 300 images, and it was originally designed for image segmentation. This dataset is challenging since many images contain multiple objects either with low contrast or touching the image boundary.

Fig. 1(c) and Fig. 1(d) show the PR curves on the DUT-OMRON [13] and SOD [12] dataset, respectively. In Fig. 1(c), DHS ranks the first over other methods with a large margin. The key reason is that DHS selected 3,500 images from DUT-OMRON dataset as the training set and we use DHS test the overall dataset.

Methods	SED1		SED2	
	F_β	MAE	F_β	MAE
Amulet	0.8917	0.06019	0.8298	0.06204
Amulet-1/1	0.8918	0.06087	0.8333	0.06104
Amulet-1/2	0.8914	0.06095	0.8327	0.06112
Amulet-1/4	0.8904	0.06124	0.8312	0.06142
Amulet-1/8	0.8871	0.06212	0.8243	0.06265
Amulet-1/16	0.8805	0.06424	0.8109	0.06695
Amulet_{BPR-}	0.8725	0.06610	0.8143	0.08651
DCL [4]	0.8546	0.15131	0.7946	0.15652
DHS [7]	0.8773	0.05404	0.8239	0.07886
DS [6]	0.8445	0.09306	0.7541	0.12330
ELD [3]	0.8715	0.06704	0.7591	0.10282
LEGS [10]	0.8542	0.10340	0.7358	0.12356
MDF [14]	0.8419	0.09893	0.8003	0.10136
RFCN [11]	0.8502	0.11662	0.7667	0.11306
BL [9]	0.7675	0.18489	0.7047	0.18564
BSCA [8]	0.8048	0.15347	0.7062	0.15784
DRFI [2]	0.8068	0.14799	0.7341	0.13336
DSR [5]	0.7909	0.15794	0.7116	0.14063

Table 1. The F-measure and MAE of different saliency detection methods on the SED dataset. The best three results are shown in red, green and blue. The proposed methods rank first or second on this dataset.

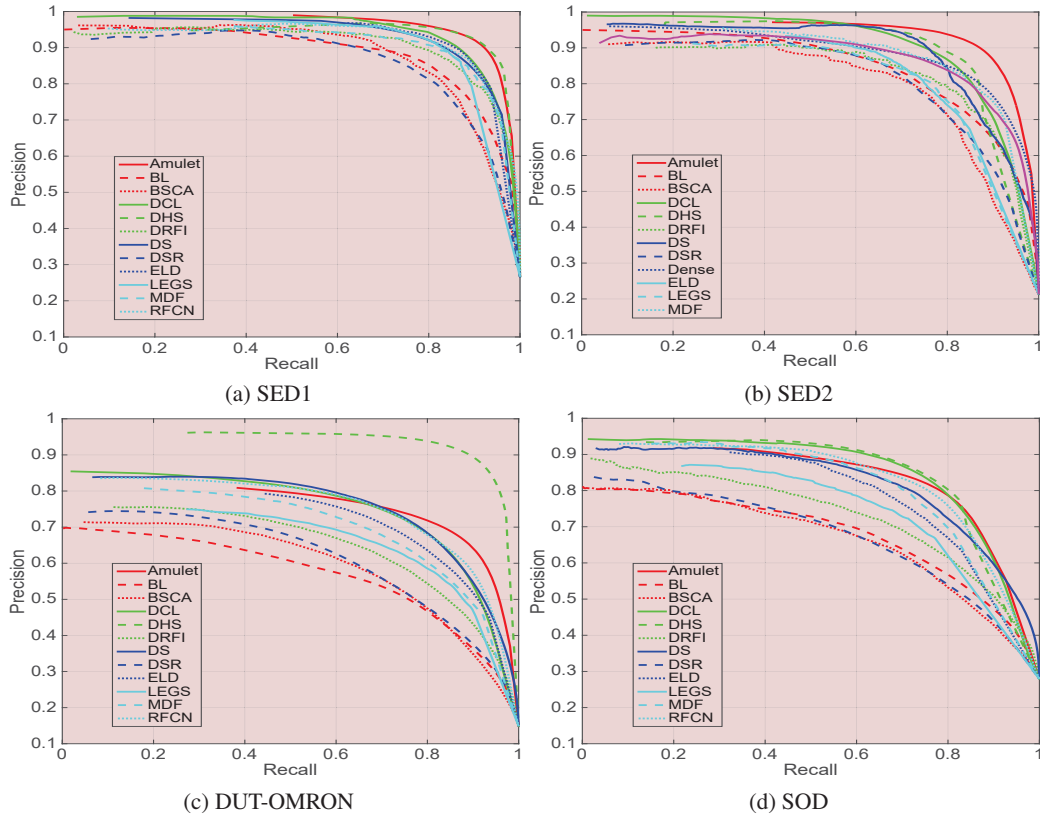


Figure 1. PR curves of the proposed algorithm and other state-of-the-art methods on the DUT-OMRON, SED and SOD datasets .

References

- [1] A. Borji. What is a salient object? a dataset and a baseline model for salient object detection. *IEEE TIP*, 24(2):742–756, 2015. 1
- [2] H. Jiang, J. Wang, Z. Yuan, Y. Wu, N. Zheng, and S. Li. Salient object detection: A discriminative regional feature integration approach. In *CVPR*, pages 2083–2090, 2013. 1
- [3] G. Lee, Y.-W. Tai, and J. Kim. Deep saliency with encoded low level distance map and high level features. In *CVPR*, pages 660–668, 2016. 1
- [4] G. Li and Y. Yu. Deep contrast learning for salient object detection. In *CVPR*, pages 478–487, 2016. 1
- [5] X. Li, H. Lu, L. Zhang, X. Ruan, and M.-H. Yang. Saliency detection via dense and sparse reconstruction. In *ICCV*, pages 2976–2983, 2013. 1
- [6] X. Li, L. Zhao, L. Wei, M.-H. Yang, F. Wu, Y. Zhuang, H. Ling, and J. Wang. Deep saliency: Multi-task deep neural network model for salient object detection. *IEEE TIP*, 25(8):3919–3930, 2016. 1
- [7] N. Liu and J. Han. Dhsnet: Deep hierarchical saliency network for salient object detection. In *CVPR*, pages 678–686, 2016. 1
- [8] Y. Qin, H. Lu, Y. Xu, and H. Wang. Saliency detection via cellular automata. In *CVPR*, pages 110–119, 2015. 1
- [9] N. Tong, H. Lu, X. Ruan, and M.-H. Yang. Salient object detection via bootstrap learning. In *CVPR*, pages 1884–1892, 2015. 1
- [10] L. Wang, H. Lu, X. Ruan, and M.-H. Yang. Deep networks for saliency detection via local estimation and global search. In *CVPR*, pages 3183–3192, 2015. 1
- [11] L. Wang, L. Wang, H. Lu, P. Zhang, and X. Ruan. Saliency detection with recurrent fully convolutional networks. In *ECCV*, pages 825–841, 2016. 1
- [12] Q. Yan, L. Xu, J. Shi, and J. Jia. Hierarchical saliency detection. In *CVPR*, pages 1155–1162, 2013. 1
- [13] C. Yang, L. Zhang, H. Lu, X. Ruan, and M.-H. Yang. Saliency detection via graph-based manifold ranking. In *CVPR*, pages 3166–3173, 2013. 1
- [14] R. Zhao, W. Ouyang, H. Li, and X. Wang. Saliency detection by multi-context deep learning. In *CVPR*, pages 1265–1274, 2015. 1